THE JOURNAL OF BIOLOGICAL CHEMISTRY VOL. 281, NO. 24, pp. 16615–16624, June 16, 2006

Identification of the Expressed Form of Human Cytosolic Phospholipase $A_2\beta$ ($cPLA_2\beta$)

*$cPLA_2\beta3$ IS A NOVEL VARIANT LOCALIZED TO MITOCHONDRIA AND EARLY ENDOSOMES**

Received for publication, February 23, 2006, and in revised form, April 12, 2006 Published, JBC Papers in Press, April 14, 2006, DOI 10.1074/jbc.M601770200

Moumita Ghosh[‡], Robyn Loper[‡], Michael H. Gelb[§], and Christina C. Leslie[‡¶1]

From the [‡]Program in Cell Biology, Department of Pediatrics, National Jewish Medical and Research Center, Denver, Colorado 80206, the [§]Departments of Chemistry and Biochemistry, University of Washington, Seattle, Washington 98195, and the [¶]Departments of Pathology and Pharmacology, University of Colorado School of Medicine, Denver, Colorado 80206

In this study, we identify the principal splice variant of human cytosolic phospholipase $A_2\beta$ ($cPLA_2\beta$) (also known as Group IVB $cPLA_2$) present in cells. In human lung, spleen, and ovary and in a lung epithelial cell line (BEAS-2B), $cPLA_2\beta$ is expressed as a 100-kDa protein, not the 114-kDa form originally predicted. Using RNA interference, the 100-kDa protein in BEAS-2B cells was confirmed to be $cPLA_2\beta$. BEAS-2B cells contain three different RNA splice variants of $cPLA_2\beta$ ($\beta1$, $\beta2$, and $\beta3$). $cPLA_2\beta1$ is identical to the previously cloned $cPLA_2\beta$, predicted to encode a 114-kDa protein. However, $cPLA_2\beta2$ and $cPLA_2\beta3$ splice variants are smaller and contain internal deletions in the catalytic domain. The 100-kDa $cPLA_2\beta$ in BEAS-2B cells is the translated product of $cPLA_2\beta3$. $cPLA_2\beta3$ exhibits calcium-dependent PLA_2 activity against palmitoyl-arachidonyl-phosphatidylethanolamine and low level lysophospholipase activity but no activity against phosphatidylcholine. Unlike Group IVA $cPLA_2\alpha$, $cPLA_2\beta3$ is constitutively bound to membrane in unstimulated cells, localizing to mitochondria and early endosomes. $cPLA_2\beta3$ is widely expressed in tissues, suggesting that it has a generalized function at these unique sites.

Phospholipase A_2 (PLA_2)[2] enzymes catalyze hydrolysis of *sn*-2 acyl chains from membrane phospholipids. They execute diverse functions, such as digestion of dietary phospholipids, microbial degradation, membrane remodeling, and production of lipid mediators. Traditionally, PLA_2s are grouped depending on their active site residues, requirements for calcium, and localization in the cell. Three main classes of PLA_2s are Group VI intracellular calcium-independent PLA_2s, low molecular weight secreted PLA_2s, and Group IV cytosolic PLA_2s (1, 2). Group IVA cytosolic $PLA_2\alpha$ has received special attention, because it is the only PLA_2 that selectively hydrolyzes arachidonic acid from the *sn*-2 position of membrane phospholipids (1). Arachidonic acid is the precursor of prostaglandins and leukotrienes (1, 3). Mice genetically deficient in $cPLA_2\alpha$ have provided evidence for its critical role in regulating physiological processes and various diseases (4–11). $cPLA_2\alpha$ contains an N-terminal calcium binding domain (C2 domain) and a C-terminal catalytic domain (12). Calcium binds to the C2 domain and facilitates the translocation of the enzyme from cytosol to the Golgi, endoplasmic reticulum, and nuclear envelope (13–16). Five other members of the Group IV $cPLA_2$ family, $cPLA_2\beta$ (Group IVB), $cPLA_2\gamma$ (Group IVC), $cPLA_2\delta$ (Group IVD), $cPLA_2\varepsilon$ (Group IVE), and $cPLA_2\zeta$ (Group IVF), have been identified (17–21). $cPLA_2\delta$, -ε, and -ζ are clustered near $cPLA_2\beta$ on mouse chromosome 2 and have more homology to $cPLA_2\beta$ than to $cPLA_2\alpha$ or $cPLA_2\gamma$ (21). From analysis of the human genome, $cPLA_2\beta$ is similarly positioned near $cPLA_2\delta$, -ε, and -ζ on chromosome 15. All members of the Group IV family have a conserved Ser/Asp dyad necessary for catalysis (12).

Human $cPLA_2\beta$ was originally cloned from human brain and pancreas cDNA libraries and predicted to encode a protein of 114 kDa (17, 18). $cPLA_2\beta$ message is ubiquitously expressed in human tissues, with strong expression in pancreas and cerebellum (17). Unlike other Group IV $cPLA_2$s, $cPLA_2\beta$ contains an N-terminal truncated JmjC domain that is immediately upstream of the C2 domain (22). Surprisingly, $cPLA_2\beta$ mRNA was found to be mostly in the unspliced form (17, 18). Preliminary enzymatic characterization of $cPLA_2\beta$ using crude lysates of cells overexpressing N-terminally truncated $cPLA_2\beta$ lacking the JmjC domain showed that $cPLA_2\beta$ has calcium-dependent PLA_2 activity, although it is much lower than that of $cPLA_2\alpha$ (17, 18). Residues necessary for catalytic activity of $cPLA_2\alpha$ (Ser^{228}, Asp^{549}, and Arg^{566}) are conserved in $cPLA_2\beta$ (Ser^{566}, Asp^{846}, and Arg^{863}) (17, 23, 24).

The original finding of abundant unspliced message raised questions about the presence of splice variants. Importantly, the endogenous protein expressed in cells has not been identified, which is the focus of this study. We found that three $cPLA_2\beta$ splice variants ($cPLA_2\beta1$, $cPLA_2\beta2$, and $cPLA_2\beta3$) are present in human lung epithelial cells (BEAS-2B), but only $cPLA_2\beta3$, which contains a C-terminal internal deletion, is translated to a 100-kDa protein. No evidence for the translation of the originally cloned $cPLA_2\beta$ mRNA was found in cells or human tissues. In this study, we also characterize the enzymatic activities, membrane binding properties, and subcellular localization of $cPLA_2\beta3$.

EXPERIMENTAL PROCEDURES

Materials—[5,6,8,9,11,12,14,15-^{3}H]Arachidonic acid (100 Ci/mmol), 1-palmitoyl-2-[^{14}C]arachidonyl-phosphatidylcholine (1-palmitoyl-2-[^{14}C]arachidonyl-PC) (48 mCi/mmol), 1-[^{14}C]palmitoyl-2-lyso-PC (55 mCi/mmol), and 1-palmitoyl-2-[^{14}C]arachidonyl-phosphatidylethanolamine (1-palmitoyl-2-[^{14}C]arachidonyl-PE) (48 mCi/mmol) were from PerkinElmer Life Sciences. 1-Palmitoyl-[^{14}C]linoleoyl-PE (55 mCi/mmol) was from Amersham Biosciences. 1-Palmitoyl-2-arachidonyl-PE and 1-palmitoyl-2-linoleoyl-PE were from Avanti Polar Lipids. 1-Palmitoyl-2-arachidonyl-PC, dioleoylglycerol, glutathione-Sepharose

* This work was supported by National Institutes of Health Grants HL34303 and HL61378 (to C. C. L.) and HL50040 (to M. H. G). The costs of publication of this article were defrayed in part by the payment of page charges. This article must therefore be hereby marked "*advertisement*" in accordance with 18 U.S.C. Section 1734 solely to indicate this fact.

The nucleotide sequence(s) reported in this paper has been submitted to the GenBank™/EBI Data Bank with accession number(s) DQ523799 for $cPLA_2\beta2$ (Group IVB2 PLA_2), and DQ523800 for $cPLA_2\beta3$ (Group IVB3 PLA_2).

[1] To whom correspondence should be addressed: Dept. of Pediatrics, National Jewish Medical and Research Center, 1400 Jackson St., Denver, CO 80206. Tel.: 303-398-1214; Fax: 303-270-2155; E-mail: lesliec@njc.org.

[2] The abbreviations used are: PLA_2, phospholipase A_2; $cPLA_2\beta$, cytosolic phospholipase $A_2\beta$; PC, phosphatidylcholine; PE, phosphatidylethanolamine; BSA, bovine serum albumin; siRNA, short interfering RNA; GST, glutathione *S*-transferase; OxPhos, oxidative phosphorylation; EEA1, early endosomal antigen 1; MRP-6, mannose 6-phosphate receptor 6; PBS, phosphate-buffered saline.

beads, bovine serum albumin (BSA), fatty acid-free BSA, Freund's adjuvant, pluronic acid, and anti-His antibody were from Sigma. cPLA$_2$ inhibitors pyrrolidine-2 and AZ-1 were synthesized as previously described (25–27). The human bronchial epithelial cell line BEAS-2B (CRL-9609) was from the American Type Culture Collection. Dulbecco's modified Eagle's medium was from Biowhittaker. Penicillin/streptomycin/L-glutamine solution was from Invitrogen. Fetal bovine serum was from Irvine Scientific. Methyl arachidonyl fluorophosphonate was purchased from Biomol, and silica gel LC-Si SPE columns were from Supelco. Affinity-purified anti-peptide antibodies were synthesized by Quality Control Biochemicals (Hopkinton, MA), and the human multiple tissue blot was purchased from Bioworld (Dublin, OH). Anti-GST antibody was from Santa Cruz Biotechnology, Inc. (Santa Cruz, CA). Protease inhibitor mixture tablets and Fugene 6 were from Roche Applied Biosciences. SMART pool siRNA and nontargeting control siRNA were from Dharmacon RNA Technologies (Dharmacon, Lafayette, CO). The total RNA isolation kit was purchased from Promega (SV Total RNA Isolation Kit), the Advantage reverse transcription-PCR kit was from Clontech, and TA cloning vector, pcDNA3.1, and pcDNA3.1-His vectors were from Invitrogen. The plasmid isolation kit and Ni^{2+}-nitrilotriacetic acid-agarose beads were from Qiagen. Affinity-purified goat anti-rabbit antibody conjugated to Texas Red was from Jackson ImmunoResearch, and monoclonal antibody to mitochondrial OxPhos complex V, subunit b, the Alexa Fluor 488-conjugated secondary antibody, lysotracker blue-white, and anti-human golgin 97 antibodies were from Molecular Probes, Inc. Monoclonal antibodies to early endosomal antigen 1 (EEA1) and mannose 6-phosphate receptor (MRP-6) were from Abcam Inc.

Cloning of cPLA$_2$β Splice Variants from BEAS-2B Cells—BEAS-2B cells were cultured in Dulbecco's modified Eagle's medium (high glucose) with 10% fetal bovine serum and 1% penicillin/streptomycin/glutamine. To clone cPLA$_2$β splice variants from BEAS-2B cells, total RNA was isolated, and 1 μg was used to generate cDNA. PCR analysis was performed using 10 μl of cDNA for cPLA$_2$β and 5 μl of cDNA for glyceraldehyde phosphate dehydrogenase following the manufacturer's instructions (Clontech Advantage reverse transcription-PCR kit). Specific primers for human cPLA$_2$β are as follows: 5′-gacgcagccatggcggaggcggctttg-3′, 5′-ctggtggcccgggagctctcctgcttg-3′, 5′-caagcaggagagctcccgggccaccag-3′, 5′-ctgcagcggtaccggcaggagctggc-3′, 5′-gccagctcctgccggtaccgctgcag-3′, 5′-gccacctgagcccgaggctctgaag-3′.

These primers were designed based on the sequence of human cPLA$_2$β (accession number AF065215) to amplify the full-length cDNA in three fragments. The PCR products were cloned into the TA cloning vector, and the fragments were sequenced and then assembled into the full-length clones (cPLA$_2$β1, cPLA$_2$β2, and cPLA$_2$β3) using the internal restriction sites present in the PCR products.

Production of Recombinant cPLA$_2$β and cPLA$_2$β Antibodies—Human cPLA$_2$β clone (designated cPLA$_2$β1 in this study) (GenBank™ accession number AF065215) was generously provided by Dr. R. Todd Pickard (Lilly) and subcloned into the baculovirus expression vectors pAcGHLT and pAcHLT in the StyI/NotI sites. Endogenous cPLA$_2$β3 cDNA was cloned into pAcHLT in the NotI/BglII sites. Sf9 cells were grown in suspension at 27 °C in TNF-FH medium as previously described (28). Recombinant baculovirus was generated by co-transfection of Sf9 cells with cPLA$_2$β constructs and linearized baculovirus DNA (Baculogold) following the manufacturer's instructions (BD Biosciences Pharmingen). Recombinant virus was generated and amplified by standard protocols. To determine expression of cPLA$_2$βs, Sf9 cells were plated in a 12-well tissue culture plate at a density of 0.5×10^6 cells/well and were infected with recombinant virus at different multiplicities of infection for 1 h. The virus-containing medium was replaced with fresh medium, and cells were incubated for 48 h. Expression of GST-cPLA$_2$β1, His$_6$-cPLA$_2$β1, and His$_6$-cPLA$_2$β3 proteins was determined by Western blot analysis using anti-GST or anti-His monoclonal antibodies.

GST-cPLA$_2$β1, His$_6$-cPLA$_2$β1, and His$_6$-cPLA$_2$β3 expressed in Sf9 cells were affinity-purified using glutathione-agarose beads or nickel-agarose beads following the manufacturer's instructions. The concentration of cPLA$_2$β enzymes in eluted fractions was determined by comparing the intensity of Coomassie-stained bands of cPLA$_2$βs on SDS-polyacrylamide gels with a standard curve made with BSA. For mammalian expression, full-length cPLA$_2$β cDNAs were cloned into the pcDNA 3.1 vector in the NheI/NotI sites or into the pcDNA3.1-His vector in the NotI/XbaI sites.

To generate polyclonal antibody to full-length cPLA$_2$β1, affinity-purified GST-cPLA$_2$β1 (50–100 μg) in complete Freund's adjuvant was injected subcutaneously into rabbits. Subsequent booster injections were carried out every 3 weeks using Freund's incomplete adjuvant. Antiserum was obtained 10 days following each injection and analyzed for cross-reactivity to cPLA$_2$β1 by Western blotting. To generate anti-peptide antibodies, the peptide (LTEEGTFKVVDEEAMEK) corresponding to a unique sequence between the truncated JmjC domain and the C2 domain of human cPLA$_2$β1 and peptides corresponding to the extreme C terminus of the predicted amino acid sequences (DYNLHGAFQGSGGHPRRRQLGR) and (EALRQAVQRRRQRRPH) of cPLA$_2$β2 and cPLA$_2$β3, respectively, were synthesized. Peptides conjugated to keyhole limpet hemocyanin carrier protein were used to produce rabbit polyclonal antibodies (Quality Control Biochemicals, Hopkinton, MA).

Western Blot Analysis—Cells were lysed in buffer containing 50 mM Hepes, pH 7.4, 150 mM sodium chloride, 1.5 mM magnesium chloride, 10% glycerol, 1% Triton X-100, 1 mM EGTA, 200 μM sodium vanadate, 10 mM tetrasodium pyrophosphate, 100 mM sodium fluoride, 300 mM *p*-nitrophenyl phosphate, 1 mM phenylmethylsulfonyl fluoride, 10 μg/ml leupeptin, and 10 μg/ml aprotinin. Lysates were centrifuged at 15,000 rpm for 15 min, and the protein concentration of the supernatant was determined by the bicinchoninic acid method. Lysates were boiled in Laemmli buffer, and 20–30 μg of total protein per lane was separated on a 10% SDS-polyacrylamide gel. Proteins were transferred onto a nitrocellulose membrane, and the membrane was blocked in Tris-buffered saline containing 0.25% Tween 20, 3% BSA, and 5% nonfat dried milk. Nitrocellulose membranes were incubated overnight at 4 °C with a 1:2500 dilution of cPLA$_2$β1 antibody or a 1:1000 dilution of anti-peptide antibodies. Immunoreactive proteins were detected using the Amersham Biosciences ECL system.

Determination of cPLA$_2$β Localization in Soluble and Particulate Fractions of BEAS-2B Cells—BEAS-2B cells were plated in a 6-well plate (1×10^5 cells/well) and transiently transfected with untagged cPLA$_2$β1 in the pcDNA3.1 vector using Fugene 6 transfection reagent. After 24 h of transfection, control and transfected cells were sonicated on ice in homogenization buffer containing 10 mM Hepes, pH 7.4, 0.34 M sucrose, 1 mM EGTA, 10% glycerol, 10 μg/ml leupeptin, 10 μg/ml aprotinin, and 1 mM phenylmethylsulfonyl fluoride with or without 5 mM $CaCl_2$. Homogenates were centrifuged at 100,000 × *g* for 1 h at 4 °C to obtain the soluble and particulate fractions. Protein concentration was determined, and the relative amount of cPLA$_2$β in each fraction was measured by Western blotting.

Knockdown of Endogenous cPLA$_2$β by RNA Interference—BEAS-2B cells were plated in a 12-well plate (0.5×10^5 cells/well) in 1 ml of Dulbecco's modified Eagle's medium containing 10% fetal bovine serum and incubated overnight at 37 °C with 5% CO_2. Cells at 50–60% con-

fluence were transfected with different concentrations of SMART pool siRNA made against human cPLA$_2\beta$1 (Refseq number NM_005090). MIRUS Trans IT-TKO transfection reagent was used to transfect siRNA and nontargeting control siRNA following the manufacturer's protocol (Mirus, Madison, WI). Cells were lysed 48 h post-transfection, and relative intensities of cPLA$_2\beta$ protein were determined by Western blotting.

Homology Model of cPLA$_2\beta$3—A homology model of cPLA$_2\beta$3 was made using the x-ray structure of cPLA$_2\alpha$ (Protein Data Bank number 1CJY) as the template (12). cPLA$_2\alpha$ and cPLA$_2\beta$3 amino acid sequences were first aligned with the ClustalW program. The model was made using the homology module of the InsightII software package (Accelrys Corp.). For segments of the cPLA$_2\alpha$ protein that align to segments of cPLA$_2\beta$3, the cPLA$_2\alpha$ residues were replaced with the corresponding cPLA$_2\beta$3 residues. No attempt was made to include cPLA$_2\beta$3 inserts (those segments that do not align to cPLA$_2\alpha$ segments).

Enzyme Assays—PLA$_2$ activity of cPLA$_2\beta$s was assayed using 1-palmitoyl-2-[^{14}C]arachidonyl-PC or 1-palmitoyl-2-[^{14}C]arachidonyl-PE as substrates. The reaction mixture (50-μl final volume) contained 30 μM phospholipid substrate (100,000 dpm/1.5 nmol) and 9 μM dioleoylglycerol (which was co-sonicated with the substrate). To prepare substrate, solvents were evaporated from the lipid mixture under a stream of nitrogen, 50 mM Hepes buffer, pH 7.4, was added, and the lipid mixture was sonicated at 4 °C for 10 s on ice using a microprobe (Braun Instruments) to form small unilamellar vesicles. A final concentration of 150 mM sodium chloride, 1 mg/ml fatty acid-free BSA, 1 mM EGTA, and 5 mM $CaCl_2$ was added to the vesicles. Reactions were started by the addition of the enzyme (250 ng to 1 μg) and incubated at 37 °C for the times indicated. Free fatty acids were extracted using Dole reagent (propan-2-ol, heptane, and 1 N H_2SO_4, 20:5:1) and separated by silicic acid chromatography as previously described using unlabeled oleic acid (25 μg) as carrier lipid (29).

Lysophospholipase activity was measured using 1-[^{14}C]palmitoyl-2-lyso-PC substrate sonicated in 50 mM Hepes, pH 7.4, to make micelles as previously described (30). Assays contained 50 μM substrate (120,000 dpm), 1 mM EGTA, and 5 mM $CaCl_2$ in a final volume of 50 μl. Reactions were started by adding affinity-purified enzyme and incubated at 37 °C for the times indicated. Free fatty acid product was extracted using Dole reagent. After vortexing, the upper heptane phase was removed and dried under a stream of nitrogen, and 0.5 ml of heptane was added. Radiolabeled free fatty acids were measured by liquid scintillation spectrometry. For inhibitor experiments, enzymes were preincubated for 2 min at 37 °C with inhibitors, and reactions were started by the addition of substrate.

Immunofluorescence Microscopy—BEAS-2B cells were plated in 35-mm glass bottom MatTek plates at a density of 1×10^5/cm^2 and incubated overnight. The cells were washed twice with PBS and incubated with ice-cold fixative containing 3.2% paraformaldehyde and 3% sucrose in PBS for 15 min. After fixation, cells were rinsed five times with PBS and permeabilized with 0.1% Triton X-100 in PBS for 15 min at room temperature. Samples were blocked for 1 h in PBS containing 10% fetal bovine serum and incubated with rabbit polyclonal antibody to full-length cPLA$_2\beta$1 (1:100) overnight, followed by incubation with goat anti-rabbit secondary antibody conjugated to Texas Red (1:200) for 1 h. For mitochondrial localization, cells were co-stained with mouse monoclonal antibody to anti-OxPhos complex V, subunit b (1:100) for 2 h, followed by anti-mouse secondary antibody conjugated to Alexa Fluor 488 (1:100) for 1 h. For localization of early or late endosomes, fixed cells were incubated (2 h) with monoclonal antibody to EEA1 or monoclonal antibody to MRP-6 (1:100), respectively. BEAS-2B cells were loaded with 1 mM lysotracker blue-white for 1 h prior to fixation for localization of lysosomes, and a monoclonal antibody to human golgin 97 was used for the identification of Golgi. For translocation of cPLA$_2\alpha$, BEAS-2B cells were transfected with GFP-cPLA$_2\alpha$, serum-starved overnight, and either left unstimulated or stimulated with 1 μM ionomycin for 15 min followed by fixation. Immunofluorescence microscopy was carried out using an inverted Zeiss 200M microscope with a 175-watt xenon lamp. Cells were visualized with a 63× oil immersion objective using Cy3 and fluorescein isothiocyanate filters. Images were acquired with a CCD camera from Sensicam, and data were analyzed using Intelligent Imaging Innovations Inc. (3I) software.

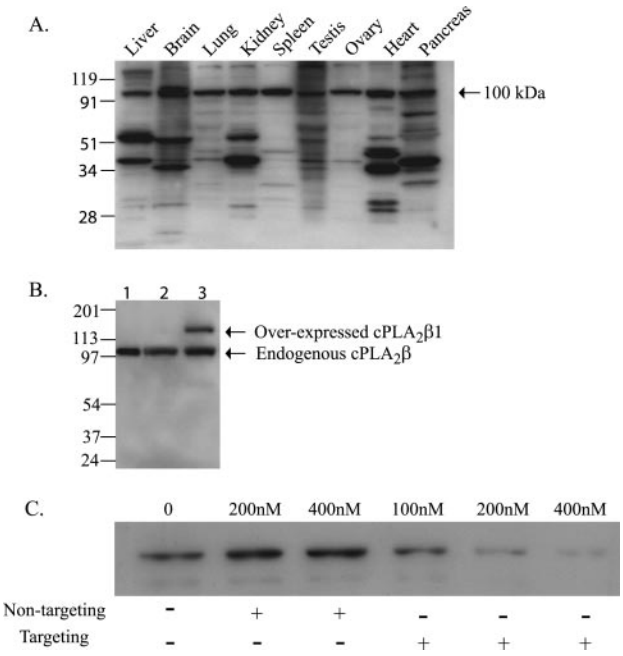

FIGURE 1. **Expression of cPLA$_2\beta$ protein in human tissues and in BEAS-2B cells.** *A*, a human multiple tissue blot was probed with antibody to cPLA$_2\beta$1 for Western blot analysis. The *numbers* on the *left* indicate the size (kDa) of protein markers. *B*, BEAS-2B lysates were probed with anti-peptide antibody to the peptide sequence unique to cPLA$_2\beta$1 (*lane 1*) or polyclonal antibody to the full-length cPLA$_2\beta$1 (*lane 2*). Lysates of BEAS-2B cells transfected with untagged cPLA$_2\beta$1 were probed with antibody to full-length cPLA$_2\beta$1 (*lane 3*). *C*, Western blot of lysates from control BEAS-2B cells or from cells transfected with different concentrations of nontargeting and targeting siRNA probed with antibody to full-length cPLA$_2\beta$1.

RESULTS

Tissue Distribution of cPLA$_2\beta$ Protein, Identification of Transcripts, and Protein Variant Expressed in BEAS-2B Cells—To identify the form of cPLA$_2\beta$ expressed in human tissues and cells, a polyclonal antibody to full-length cPLA$_2\beta$1 was generated. Western blot analysis revealed a 100-kDa protein that was present in all tissues (Fig. 1*A*). In some tissues (lung, spleen, and ovary), the 100-kDa protein was the predominant band detected (Fig. 1*A*). In other tissues, prominent lower molecular weight bands were also observed in the 40–60-kDa range. The lower molecular weight proteins and the 100-kDa band were not observed when blots were probed only with secondary antibody. The 100-kDa protein detected with antibody to cPLA$_2\beta$ is smaller than the 114-kDa product predicted from the previously cloned open reading frame of cPLA$_2\beta$1, suggesting that a different splice variant of cPLA$_2\beta$ is expressed in cells.

Based on the human tissue blot analysis showing that lung primarily expresses a 100-kDa form of cPLA$_2\beta$ and results of an earlier study revealing that BEAS-2B human bronchial epithelial cells express the mRNA for cPLA$_2\beta$ (31), we chose this cell line for further study of

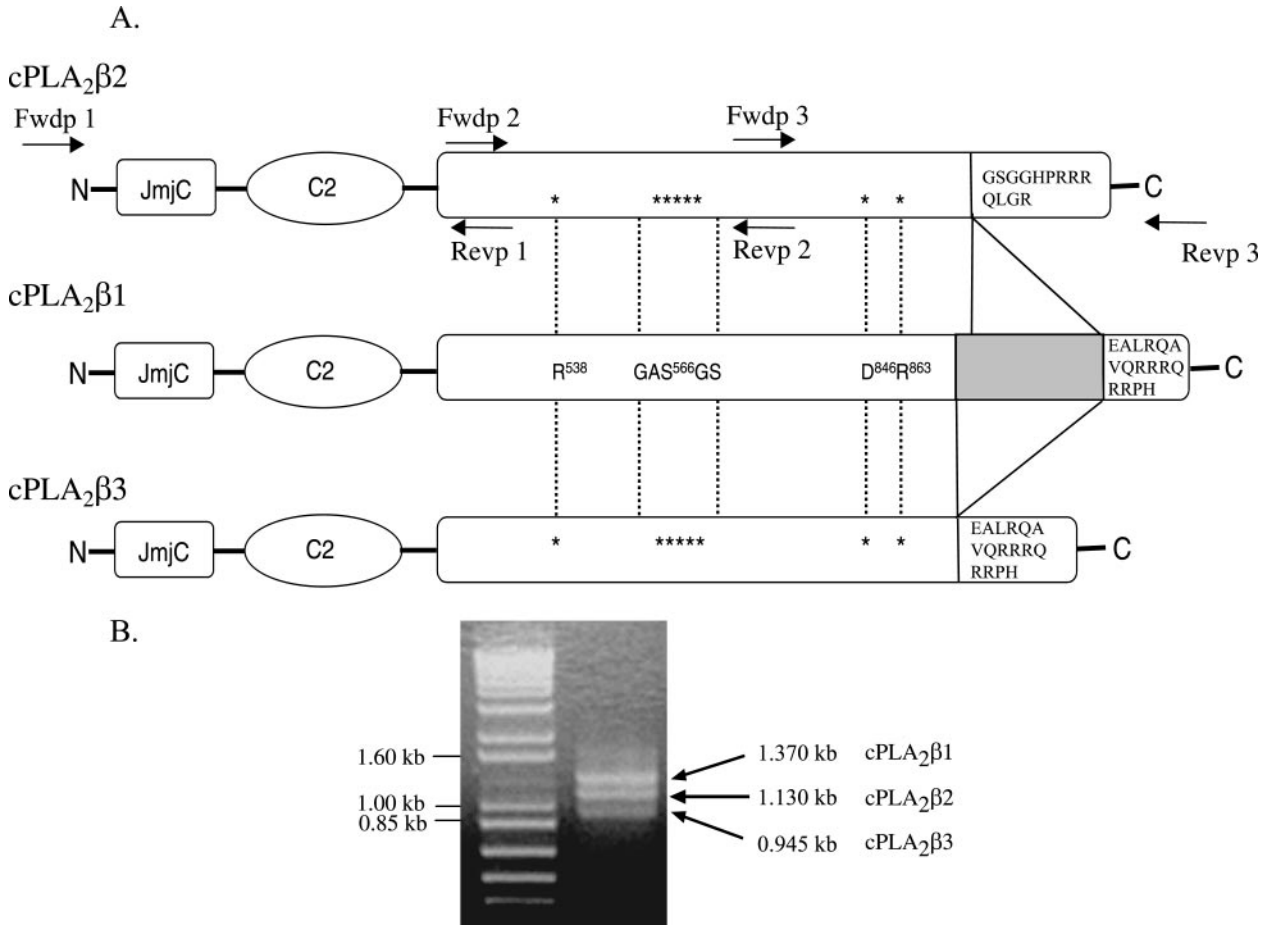

FIGURE 2. **Reverse transcription-PCR analysis of BEAS-2B cells and identification of endogenous cPLA$_2$β.** *A*, regions of cPLA$_2$β amplified by PCR analysis using the indicated primers are shown in the *diagram*. The region in cPLA$_2$β1 that is absent in cPLA$_2$β2 and cPLA$_2$β3 is *shaded gray*. Catalytic residues are shown by *asterisks*. *B*, PCR products were generated from BEAS-2B cDNA using Fwdp3 and Revp3 primer pairs. The *numbers* on the *left* indicate sizes of DNA markers, and *numbers* on the *right* show sizes of PCR products.

endogenous cPLA$_2$β. The expression of cPLA$_2$β in BEAS-2B cells was evaluated by Western blotting using an antibody to full-length cPLA$_2$β1 and an anti-peptide antibody generated to a peptide corresponding to a sequence unique to cPLA$_2$β that is between the truncated JmjC domain and the C2 domain. The anti-peptide antibody (Fig. 1*B*, *lane 1*) and antibody to full-length cPLA$_2$β1 (Fig. 1*B*, *lane 2*) exclusively detect a 100-kDa protein in BEAS-2B lysates. When transfected into BEAS-2B cells, untagged cPLA$_2$β1 is expressed as a 114-kDa protein, clearly larger than the endogenous form of cPLA$_2$β (Fig. 1*B*, *lane 3*). The antibody to full-length cPLA$_2$β1 and the anti-peptide antibody were confirmed not to cross-react with cPLA$_2$α. Western blot analysis of BEAS-2B lysate using antibody to cPLA$_2$α revealed that cPLA$_2$α migrates just below 100 kDa and was clearly separated from the 100-kDa band detected with antibodies to cPLA$_2$β. In addition, recombinant affinity-purified human cPLA$_2$α was not detected by antibodies to cPLA$_2$β by Western blotting.

To provide additional evidence that the 100-kDa form in BEAS-2B cells is endogenous cPLA$_2$β, RNA interference was used. BEAS-2B cells were transfected with SMART pool siRNA based on the cPLA$_2$β1 sequence and nontargeting control siRNA. Western blot analysis of whole cell lysates prepared 48 h post-transfection showed a concentration-dependent knockdown of the 100-kDa protein with targeting siRNA, whereas nontargeting control siRNA had no effect (Fig. 1*C*). Analysis of the same samples revealed no change in the level of cPLA$_2$α (data not shown). The RNA interference experiments support the Western blot finding that the 100-kDa protein in BEAS-2B cells is cPLA$_2$β.

Cloning of cPLA$_2$β from BEAS-2B Cells—To determine the basis for the lower molecular weight of cPLA$_2$β, reverse transcription-PCR of total RNA from BEAS-2B cells was carried out using specific primers (sequences described under "Experimental Procedures") designed based on the cPLA$_2$β1 sequence (AF065215) (17). Three forward and reverse primers were used; Fwdp1 is in the 5′-untranslated region sequence covering the Kozak sequence and the start codon (Fig. 2*A*). The reverse primer (Revp3) is in the 3′-untranslated region sequence 105 bp downstream of the stop codon. The internal primers (Fwdp2, Fwdp3, Revp1, and Revp2) were designed to produce overlapping fragments and to take advantage of existing unique restriction sites present in the cPLA$_2$β1 sequence. Single PCR products were obtained using Fwdp1/Revp1 and Fwdp2/Revp2 primer pairs (data not shown). These PCR products were gel-purified, sequenced, and found to be exact matches to AF065215. However, PCR using the Fwdp3/Revp3 primer pair resulted in three products (1.37, 1.13, and 0.95 kb), as shown in Fig. 2*B*. Sequencing of these products revealed that cPLA$_2$β exists as three distinct splice variants in BEAS-2B cells. The 1.37-kb fragment is an exact match to AF065215 (cPLA$_2$β1), but the 1.13-kb (cPLA$_2$β2) and 0.945-kb (cPLA$_2$β3) fragments have internal deletions (Fig. 2*A*). cPLA$_2$β2 is missing exon 23 (bp 2656–2841), which causes a frameshift resulting in an altered C-terminal amino acid translation, as indicated in Fig. 2*A*. cPLA$_2$β3 has a deletion (bp 2630–3002) that is in frame with cPLA$_2$β1. Consequently, the predicted C-terminal amino acid sequence of cPLA$_2$β3 is identical to the last 16 amino acids of the C terminus of

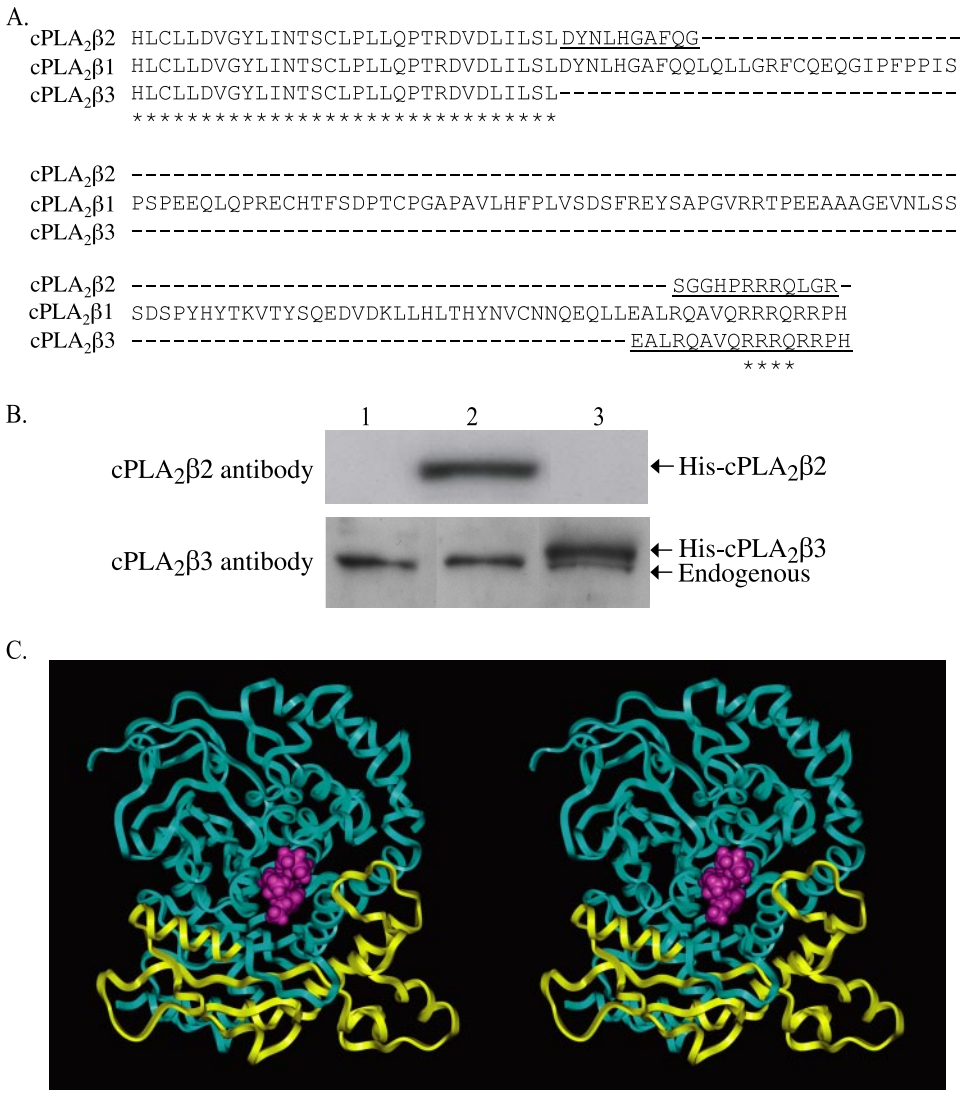

FIGURE 3. **C-terminal sequences of cPLA$_2$β splice variants and identification of cPLA$_2$β3 in BEAS-2B cells.** *A*, the multiple sequence alignment program (T-coffee) from the Expasy proteomic server was used to align the amino acid sequences at the C terminus of cPLA$_2$β1, -β2, and -β3. Amino acids identical in the three proteins are shown by *asterisks*. *Underlined* amino acids represent the residues used to raise the anti-peptide antibodies to cPLA$_2$β2 and -β3. *B*, lysates of non-transfected BEAS-2B cells (*lane 1*) and BEAS-2B cells transfected with His$_6$-cPLA$_2$β2 (*lane 2*) and with His$_6$-cPLA$_2$β3 (*lane 3*) were analyzed by Western blotting using anti-peptide antibodies generated to the predicted C termini of cPLA$_2$β2 or cPLA$_2$β3. *C*, stereo view of the catalytic domain of cPLA$_2$α taken from the x-ray structure. The segment of cPLA$_2$α (residues 590–709) that corresponds to the segment of cPLA$_2$β1 that is deleted in cPLA$_2$β3 is *colored yellow*. The α-helical lid that covers the active site slot (residues 415–432 of cPLA$_2$α) has been removed for viewing the substrate in the active site. A portion of cPLA$_2$α substrate, 1-palmitoyl-2-arachidonyl-*sn*-glycero-3-PC, has been modeled into the active site slot by placing its enzyme-susceptible *sn*-2 ester in a position next to the hydroxyl group of Ser^{228} of cPLA$_2$α (Ser^{566} of cPLA$_2$β3) so that nucleophilic attack is possible. Only the first six carbons of the *sn-1* palmitoyl chain and the first eight carbons of the *sn*-2 arachidonyl chain are shown in *purple* (substrate is shown as its van der Waals surface).

cPLA$_2$β1 (Fig. 2*A*). The calculated mass of the cPLA$_2$β2 protein is 100.6 kDa, and the calculated mass of cPLA$_2$β3 is 100.2 kDa. Interestingly, despite the deletions shown in Fig. 2*A*, all of the important catalytic residues (Arg^{538}, Ser^{566}, Asp^{846}, and Arg^{863}) are present in the predicted amino acid sequence cPLA$_2$β2 and cPLA$_2$β3 (Fig. 2*A*).

Expression of cPLA$_2$β Splice Variants in BEAS-2B Cells—To determine if one or both cPLA$_2$β splice variants are translated in BEAS-2B cells, peptides corresponding to the unique sequences (*underlined* in Fig. 3*A*) of the C termini of cPLA$_2$β2 and cPLA$_2$β3 were used to produce specific antibodies. To confirm the specificity of the antibodies and to identify the endogenous form of cPLA$_2$β, cPLA$_2$β2 and cPLA$_2$β3 were cloned and overexpressed as His$_6$-tagged proteins in BEAS-2B cells. Analysis of whole cell lysates by Western blotting demonstrated that the anti-peptide antibody specific for cPLA$_2$β3 recognized the endogenous protein as well as overexpressed His$_6$-cPLA$_2$β3 (Fig. 3*B*). The small size difference between endogenous and the overexpressed protein is due to the presence of the N-terminal His$_6$ tag. The anti-peptide antibody to the C terminus of cPLA$_2$β2 only recognized overexpressed His$_6$-cPLA$_2$β2 and not endogenous cPLA$_2$β. These results clearly demonstrate that cPLA$_2$β3 is the 100-kDa endogenous cPLA$_2$β expressed in BEAS-2B cells and also explains why endogenous cPLA$_2$β migrates faster on the gel compared with cPLA$_2$β1 (Fig. 1*B*).

Enzymatic Properties of cPLA$_2$β Enzymes—Previous enzymatic analysis of cPLA$_2$β revealed low PLA$_2$ activity, although assays were done with crude cell lysates from cells transfected with N-terminally truncated cPLA$_2$β1 lacking the truncated JmjC domain (17, 18). Because endogenous cPLA$_2$β3 contains a deletion in the catalytic domain beginning 9 amino acids after a conserved Arg residue (Arg^{863}) predicted to be important for catalytic activity (Fig. 3*A*), it was important to explore whether cPLA$_2$β3 was enzymatically active.

We began this analysis by constructing a homology model of cPLA$_2$β3 using the x-ray structure of cPLA$_2$α as a template (see "Experimental Procedures") (12). cPLA$_2$β3 contains an insert of 120 amino acids that connects the C2 and catalytic domain in contrast to cPLA$_2$α, which has a small linker of 5 amino acids. Because of these differences, no attempt was made to position the C2 domain of cPLA$_2$β3 with respect to the catalytic domain. Alignment of the catalytic domains of the two enzymes reveals 30% identities and 47% similarities in amino acid residues with no gaps or inserts of more than 7 amino acids. Thus, it is reasonable to assume that the two catalytic domains share a similar overall protein fold. Since the x-ray structure of cPLA$_2$α is known, we visualized the peptide segment that is missing in cPLA$_2$β3 relative to cPLA$_2$β1 in the context of the cPLA$_2$α structure, and this is shown in Fig. 3*C*. Structural modeling suggests that removal of this segment leads

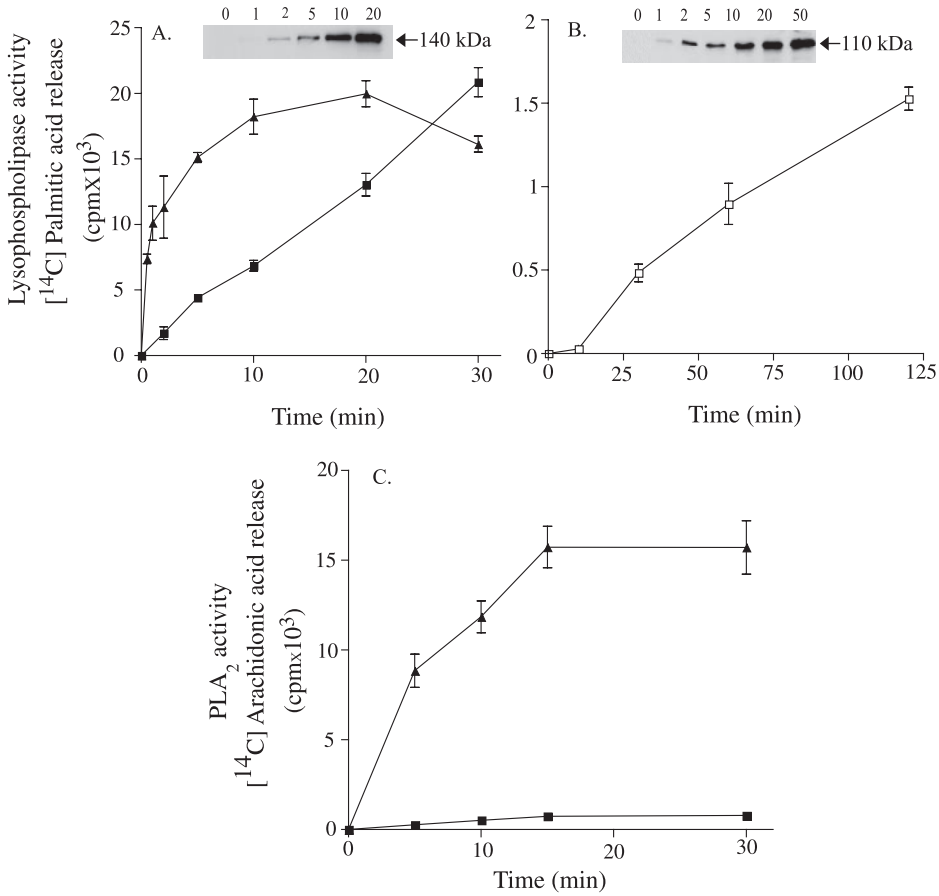

FIGURE 4. **Lysophospholipase and PLA$_2$ activities.** Lysophospholipase activity of affinity-purified cPLA$_2$β1 (■) and cPLA$_2$α (▲) (*A*) and cPLA$_2$β3 (□) (*B*) (all at 250 ng) was assayed using 1-[^{14}C]palmitoyl-2-lyso-PC (50 μM) for the indicated times. Expression of GST-cPLA$_2$β1 and His$_6$-cPLA$_2$β3 in Sf9 cells infected with increasing volumes (μl) of baculovirus is shown in the *insets* of *A* and *B*, respectively. *C*, PLA$_2$ activities of cPLA$_2$β1 (■) and cPLA$_2$α (▲) were measured at the indicated time points using 1-palmitoyl-2-[^{14}C]arachidonyl-PC (30 μM) as described under "Experimental Procedures." Results are the average of four individual experiments ± S.E.

to the deletion of a loop that forms one wall of the active site slot, a significant structural alteration that could potentially affect the enzymatic properties of cPLA$_2$β3 (Fig. 3*C*).

Group IVA cPLA$_2$α and Group IVC cPLA$_2$γ have high lysophospholipase activity (28, 30), but lysophospholipase activity of cPLA$_2$β1 had not previously been measured. Lysophospholipase activity of affinity-purified cPLA$_2$β1, cPLA$_2$β3, and cPLA$_2$α expressed in Sf9 cells was compared. The direct comparison of cPLA$_2$β1 and cPLA$_2$β3 would reveal how the deletion in the catalytic domain of β3 affects its enzymatic activity, since the variants are otherwise identical. GST-cPLA$_2$β1 and His$_6$-cPLA$_2$β3 were expressed in Sf9 cells as proteins of the predicted molecular weight as shown in the *insets* of Fig. 4, *A* and *B*. cPLA$_2$β1 hydrolyzes 1-palmitoyl-2-lyso-PC with linear kinetics up to 30 min (Fig. 4*A*). In contrast, cPLA$_2$α exhibits nonlinear kinetics as previously reported (30). Despite the deletion, cPLA$_2$β3 is enzymatically active, although based on the initial velocities, lysophospholipase activity for cPLA$_2$β3 is about 80-fold lower than that of cPLA$_2$β1 (Fig. 4*B*). When compared under the same assay conditions, affinity-purified GST-cPLA$_2$β1 and His$_6$-cPLA$_2$β1 have comparable activity, indicating that activity is not influenced by the nature of the N-terminal tag (data not shown).

The PLA$_2$ activity of cPLA$_2$β1, cPLA$_2$β3, and cPLA$_2$α was measured using 1-palmitoyl-2-arachidonyl-PC vesicles (Fig. 4*C*). cPLA$_2$β1 exhibited very low PLA$_2$ activity compared with cPLA$_2$α, whereas PLA$_2$ activity of cPLA$_2$β3 was not detected using the PC substrate. PLA$_2$ activity was also measured with 1-palmitoyl-2-arachidonyl-PE as substrate. Both cPLA$_2$β1 and cPLA$_2$β3 hydrolyzed PE with similar specific activities (Fig. 5*A*). cPLA$_2$β3 was also active against 1-palmitoyl-2-linoleoyl-PE, although it was slightly lower than against 1-palmitoyl-2-arachidonyl-PE. Specific activities of cPLA$_2$β1 and cPLA$_2$β3 are summarized in Table 1. PLA$_2$ activity of cPLA$_2$β3 was evaluated in the presence and absence of calcium using 1-palmitoyl-2-arachidonyl-PE as the substrate. The PLA$_2$ activity of cPLA$_2$β3 was largely dependent on calcium (Fig. 5*B*). However, a low level of calcium-independent activity was observed at 30 min, which was ~9% of the activity observed in the presence of calcium.

The sensitivity of cPLA$_2$β1 and cPLA$_2$β3 to cPLA$_2$α inhibitors was evaluated using the lysophospholipase assay. Pyrrolidine-2 inhibited cPLA$_2$α activity with an IC$_{50}$ of 0.01 μM, as reported previously (25) but only weakly inhibited cPLA$_2$β1 activity (IC$_{50}$ ≈ 80 μM) (Fig. 6*A*). Pyrrolidine-2 did not inhibit the activity of cPLA$_2$β3 (data not shown). Two potent inhibitors, of cPLA$_2$α AZ-1 and methyl arachidonyl fluorophosphonate, only weakly inhibited the activity of cPLA$_2$β1 (Fig. 6*B*). AZ-1 inhibited cPLA$_2$β1 with an IC$_{50}$ of 25 μM compared with an IC$_{50}$ of 0.03 μM for cPLA$_2$α as previously reported (26). For methyl arachidonyl fluorophosphonate, 50% inhibition of cPLA$_2$α occurs using a mole fraction of 0.05 (32) compared with a mole fraction of 0.7 for 50% inhibition of cPLA$_2$β1. Neither compound inhibited the lysophospholipase activity of cPLA$_2$β3.

Membrane Association of Endogenous cPLA$_2$β3—The calcium-dependent PLA$_2$ activity of affinity-purified cPLA$_2$β3 suggested a functional role for the C2 domain in binding lipid vesicles. To determine if calcium regulated cellular membrane association of cPLA$_2$β3, BEAS-2B cells were homogenized in buffer containing excess EGTA or calcium, and the localization of cPLA$_2$β3 in the 100,000 × *g* particulate or soluble fractions was determined. In cells homogenized in the presence of EGTA, endogenous cPLA$_2$β3 was only detected in the soluble fraction. However, when cells were homogenized in the presence of 5 mM calcium, most of the endogenous cPLA$_2$β3 associated with the particulate fraction (Fig. 7*A*). Surprisingly, untagged cPLA$_2$β1 transfected into

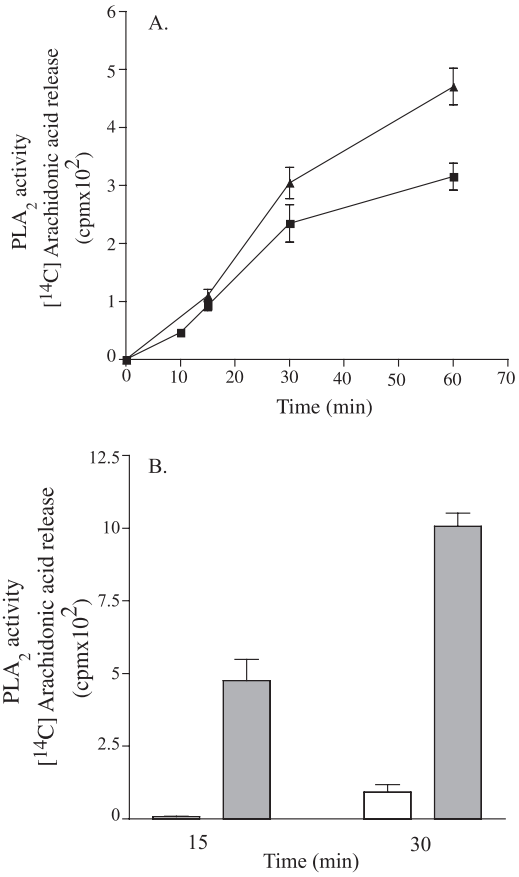

FIGURE 5. **PLA$_2$ activity of cPLA$_2\beta$ enzymes using PE substrate and role of calcium.** *A*, PLA$_2$ activity of cPLA$_2\beta$1 (■) and cPLA$_2\beta$3 (▲) was measured using 1-palmitoyl-[^{14}C]arachidonyl-PE. Results are the average of three experiments ± S.D. *B*, PLA$_2$ activity of cPLA$_2\beta$3 was measured with 1-palmitoyl-[^{14}C]arachidonyl-PE in the absence (1 mM EGTA) (*open bars*) or presence (1 mM EGTA with 5 mM $CaCl_2$) of calcium (*gray bars*). Results are the average of two independent experiments ± S.D.

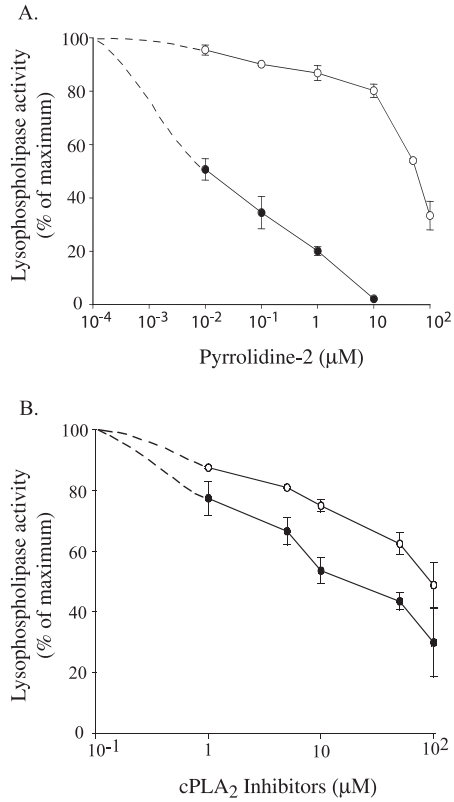

FIGURE 6. **Effect of inhibitors on lysophospholipase activity.** *A*, GST-cPLA$_2\alpha$ (●) and GST-cPLA$_2\beta$1 (○) were incubated with the indicated amount of pyrrolidine-2 for 2 min at 37 °C followed by the addition of the substrate. *B*, GST-cPLA$_2\beta$1 was incubated with the indicated amount of AZ-1 (●) and methyl arachidonyl fluorophosphonate (○) for 2 min at 37 °C followed by the addition of the substrate. Results represent the average of four independent experiments ± S.D.

TABLE 1

Lysophospholipase and PLA$_2$ activities of affinity-purified GST-cPLA$_2\beta$1 and His$_6$-cPLA$_2\beta$3

Lysophospholipase and PLA$_2$ activities of affinity-purified GST-cPLA$_2\beta$1 and His$_6$-cPLA$_2\beta$3 were investigated with different substrates as described under "Experimental Procedures" and "Results." Values represent the average of three independent experiments ± S.E. ND, not detected.

Substrate	cPLA$_2\beta$1	cPLA$_2\beta$3
	nmol/min/mg	*nmol/min/mg*
1-[^{14}C]16:0–2-lyso-PC	140.0 ± 2.05	1.6 ± 0.27
1–16:0–2-[^{14}C]20:4-PC	2.1 ± 1.1	ND
1–16:0–2-[^{14}C]20:4-PE	0.6 ± 0.09	0.8 ± 0.1
1–16:0–2-[^{14}C]18:2-PE		0.3 ± 0.064

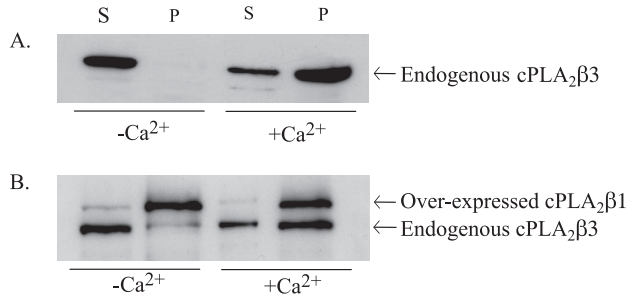

FIGURE 7. **Role of calcium in membrane association of cPLA$_2\beta$ enzymes.** BEAS-2B cells (nontransfected) (*A*) or BEAS-2B cells transfected with untagged cPLA$_2\beta$1 (*B*) were homogenized by sonication in the presence of 1 mM EGTA or 1 mM EGTA with 5 mM $CaCl_2$. Lysates were centrifuged at 100,000 × *g*, and the relative levels of cPLA$_2\beta$ enzymes in the soluble (*S*) and particulate (*P*) fractions were determined by Western blotting.

BEAS-2B cells associated with the particulate fraction in cells homogenized either in the presence or absence of calcium (Fig. 7*B*).

Subcellular Localization of Endogenous cPLA$_2\beta$3—Our results suggest that the C2 domain of cPLA$_2\beta$3 may mediate Ca^{2+}-dependent binding to the membrane. Experiments were carried out to determine if an increase in intracellular calcium levels in BEAS-2B cells induces translocation of cPLA$_2\beta$3 to membrane and to identify the subcellular membrane targeted by cPLA$_2\beta$3. To quiesce BEAS-2B cells, they were serum-starved overnight and then left either unstimulated or stimulated with 1 μM ionomycin for 15 min before fixation. As shown in Fig. 8, cPLA$_2\beta$3 was localized to membrane in serum-starved BEAS-2B cells that were not subsequently stimulated with ionomycin. Stimulation with calcium ionophore had no effect on this pattern of constitutive membrane localization of cPLA$_2\beta$3 (not shown). cPLA$_2\beta$3 localized to tubular membranes that extended from the perinuclear region to the cell periphery (Fig. 8*A*). These membrane tubules were confirmed to be mitochondria by using antibody to the marker protein OxPhos complex V, subunit b (Fig. 8*B*) (33). An overlay showed co-localization (*yellow*) of cPLA$_2\beta$3 and the mitochondrial marker to the tubular membranes (Fig. 8*C*). A deconvoluted image of the overlay clearly revealed that cPLA$_2\beta$3 also localized to vesicular structures (*red*) that did not co-localize with the mitochondrial marker (Fig. 8*D*). These vesicles clustered to the one side of the nucleus (Fig. 8*E*). They were identified as early endosomes by using antibodies to the marker EEA1 (Fig. 8*F*), which co-localized with cPLA$_2\beta$3 (*yellow*) (Fig. 8*G*) (34). Late endosomes also clustered near the nucleus as visualized using antibody to MRP-6 (Fig. 8*H*); however, there was only limited co-localization of cPLA$_2\beta$3 with the late endosome marker (Fig. 8*I*) (35). We have previously observed that Group IVA

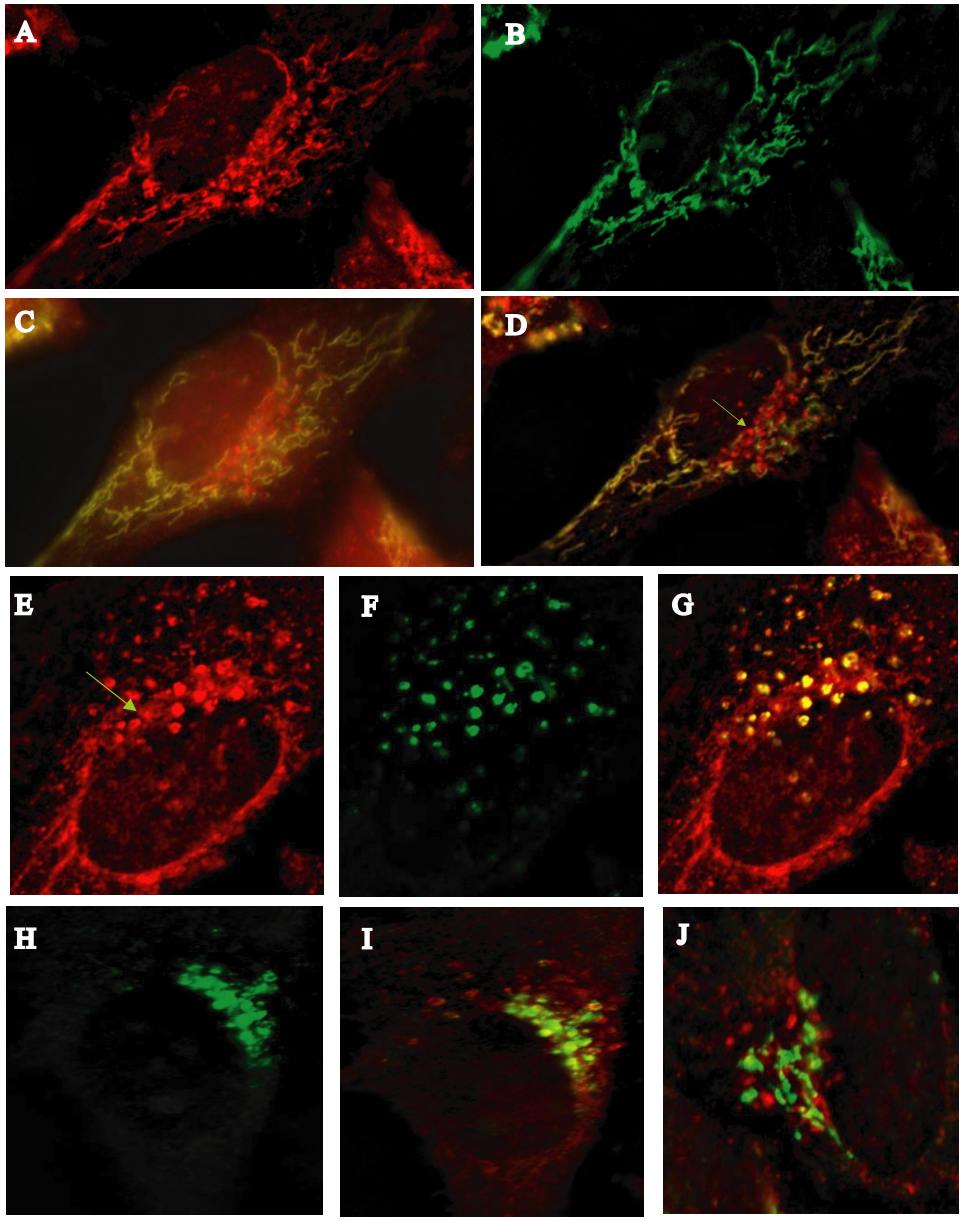

FIGURE 8. **Endogenous cPLA$_2$β3 localizes to mitochondria and early endosomes.** BEAS-2B cells were serum-starved overnight, fixed, and probed with polyclonal antiserum to cPLA$_2$β1 and monoclonal antibodies to mitochondrial marker protein OxPhos complex V, subunit b, EEA1, MRP-6, and human golgin 97. Anti-rabbit antibody conjugated to Texas Red and anti-mouse antibody conjugated to Alexa Fluor 488 were used as secondary antibodies for polyclonal and monoclonal primary antibodies, respectively. Immunofluorescence of cPLA$_2$β3 (*A*) and mitochondrial marker OxPhos complex V (*B*) are shown. An overlay of cPLA$_2$β3 fluorescence (*red*) and mitochondrial marker (*green*) is shown in *C*, and a deconvoluted image of the overlay is shown in *D*. Immunofluorescence of cPLA$_2$β3 (*red*) and EEA1 (*green*) and overlay of EEA1 with cPLA$_2$β3 are shown in *E–G*, respectively. Single staining with antibody to the late endosome marker MRP-6 and overlay of cPLA$_2$β3 with MRP-6 are shown in *H* and *I*, respectively. An overlay of a deconvoluted image of cPLA$_2$β3 and Golgi marker golgin 97 (*J*) shows that cPLA$_2$β3 is not associated with Golgi.

cPLA$_2$α localizes to Golgi upon cell stimulation; however, there was no co-localization of cPLA$_2$β3 with the Golgi marker golgin 97 (Fig. 8*J*) (16, 36). cPLA$_2$β3 also did not localize to lysosomes, which were analyzed with lyso tracker (data not shown). Using preimmune serum instead of polyclonal antiserum against cPLA$_2$β3 as well as secondary antibodies alone as controls showed only a low level of background fluorescence (data not shown). The results demonstrate that cPLA$_2$β3 is constitutively associated with mitochondria and early endosomes even in serum-starved unstimulated BEAS-2B cells. This suggests that cPLA$_2$β3, unlike cPLA$_2$α constitutively, binds to membrane at resting levels of intracellular calcium. This is supported by data showing that in contrast to cPLA$_2$β3, GFP-cPLA$_2$α expressed in BEAS-2B cells is cytosolic in serum-starved cells and translocates to Golgi and the perinuclear region in response to stimulation by calcium ionophore (data not shown).

DISCUSSION

cPLA$_2$β was cloned several years ago, but very little is known about its properties. The originally cloned cDNA was predicted to encode a protein of 114 kDa (17, 18). However, the majority of expressed sequence tags and cDNA fragments of cPLA$_2$β contained intronic sequences (17, 18). The reason for the predominance of unspliced cPLA$_2$β cDNA is not known, but it raised the possibility that multiple splice variants exist. Increasing evidence indicates that alternate splicing and exon skipping are major contributors to protein diversity in humans; therefore, it is important to identify the endogenously expressed protein variants in cells and tissues (37–43). In this study, we describe the identification and characterization of endogenous cPLA$_2$β protein, which is derived from a novel splice variant of the cPLA$_2$β gene. Human lung epithelial cells (BEAS-2B) contain three RNA splice variants of cPLA$_2$β (β1, β2, and β3). Surprisingly, no intronic sequences were found in any of these splice variants. Whereas the cPLA$_2$β1 splice variant perfectly matches the originally cloned cDNA, both cPLA$_2$β2 and cPLA$_2$β3 contain internal deletions in the catalytic domain, resulting in smaller proteins of ~100 kDa.

Our data demonstrate that BEAS-2B cells exclusively express the 100-kDa cPLA$_2$β3 splice variant rather than the 114-kDa form of cPLA$_2$β originally described (17, 18). In addition to BEAS-2B cells, we analyzed human primary skeletal muscle cells, human skin fibroblasts,

and primary monocyte derived macrophages, and in each case the expression of a 100-kDa cPLA$_2\beta$ protein was observed. Probing a panel of human tissues with antibody to full-length cPLA$_2\beta$ revealed that all human tissues express a 100-kDa cPLA$_2\beta$ protein, and is the predominant form in lung, spleen, and ovary. Prominent lower molecular weight proteins were also observed in several tissues (liver, brain, kidney, heart, and pancreas), suggesting that other splice variants of cPLA$_2\beta$ are also present. Full-length cPLA$_2\beta$ contains a truncated JmjC domain at the N terminus of the protein that is linked to the C2 and catalytic domains (22). Interestingly, a data base search has revealed the presence of an IMAGE clone (BC025290) that is homologous to the N-terminal segment of cPLA$_2\beta$ but contains additional sequence that forms a complete JmjC domain but lacks the C2 and catalytic domains. Examination of the genomic sequence of human chromosome 15 reveals that this IMAGE clone is derived from the first eight exons of cPLA$_2\beta$, after which it stops prematurely and thus lacks the C2 and catalytic domains. From analysis of the cDNA sequence of full-length cPLA$_2\beta$, the truncation of the JmjC domain is due to the skipping of exons 7 and 8. The N-terminal short variant of cPLA$_2\beta$ (BC025290) containing the complete JmjC domain is predicted to encode a protein of ~35 kDa and may represent one of the smaller proteins detected in some tissues with antibody to cPLA$_2\beta$. JmjC domains, part of the cupin metalloenzyme superfamily, have a β-barrel structure and are often found in nuclear proteins that regulate chromatin stability (44–47). Recent evidence suggests that JmjC proteins are 2-oxoglutarate-Fe(II)-dependent dioxygenases (44). Full-length cPLA$_2\beta$ lacks the C-terminal region of the JmjC domain, which contains one of the three conserved metal-binding residues of a complete JmjC domain, suggesting that it lacks the dioxygenase activity. These data suggest that cPLA$_2\beta$ undergoes complex splicing regulation, which potentially results in the production of functionally diverse protein products.

Comparisons of the enzymatic activity of cPLA$_2\beta$1 and cPLA$_2\beta$3 provided insight into the effect of the modified catalytic domain of cPLA$_2\beta$3 on its properties. Activity assays of affinity-purified cPLA$_2\beta$3 with palmitoyl-lyso-PC substrate demonstrate that despite the striking change in the structure, this enzyme is active but has lower activity than cPLA$_2\beta$1. Interestingly, cPLA$_2\beta$1 and cPLA$_2\beta$3 exhibited comparable PLA$_2$ activity and preferentially hydrolyzed palmitoyl-arachidonyl-PE but exhibited little or no activity with palmitoyl-arachidonyl-PC. Of the cPLA$_2\alpha$ inhibitors tested, only AZ-1 was effective at inhibiting cPLA$_2\beta$1 but had no effect on cPLA$_2\beta$3, indicating that the deletion in cPLA$_2\beta$3 affects enzymatic properties and susceptibility to inhibitors. However, the deletion in cPLA$_2\beta$3 did not have a generalized effect but rather specifically affected its action on certain substrates. The actual endogenous substrate for cPLA$_2\beta$3 has not been identified and may be unique to its novel site of localization. Additionally, factors such as post-translational modification and possibly binding proteins may play a role in regulating cPLA$_2\beta$3 activity.

All Group IV PLA$_2$s with the exception of cPLA$_2\gamma$ contain C2 domains, which generally function to promote calcium-dependent membrane binding (17–21, 48–50). The PLA$_2$ activity of cPLA$_2\beta$3 against phosphatidylethanolamine is significantly enhanced by calcium, suggesting a functional role for the C2 domain; however, unlike cPLA$_2\alpha$, cPLA$_2\beta$3 exhibits significant calcium-independent activity against PE substrate. Although C2 domains of cPLA$_2\alpha$ and cPLA$_2\beta$3 have the same topological fold, they share only 25% amino acid identity. Of the seven important Ca^{2+}-binding residues of cPLA$_2\alpha$, only four are conserved in cPLA$_2\beta$3 (51, 52). Moreover, cPLA$_2\beta$3 lacks important hydrophobic residues found in the cPLA$_2\alpha$ calcium-binding loops that are important for binding to PC vesicles (53–56). This may contribute to the poor activity of cPLA$_2\beta$3 with PC substrate. Another interesting structural difference between cPLA$_2\alpha$ and cPLA$_2\beta$3 is that the C2 domain of cPLA$_2\alpha$ is connected to the catalytic domain by a flexible linker of 5 amino acids that may undergo rotational changes affecting the interaction of the catalytic domain to the membrane (12), whereas in cPLA$_2\beta$3 this linker is 120 amino acids long. This suggests potential differences in membrane binding properties of cPLA$_2\beta$3 and cPLA$_2\alpha$. Our results demonstrate differences in the partitioning of cPLA$_2\beta$1 and cPLA$_2\beta$3 into soluble and particulate fractions of BEAS-2B homogenates prepared in excess calcium or EGTA. Since the C2 domains of cPLA$_2\beta$1 and cPLA$_2\beta$3 are homologous, the results indicate that the deletion in the C terminus of cPLA$_2\beta$3 affects its membrane binding properties, perhaps due to conformational affects.

A surprising finding was that cPLA$_2\beta$3 is constitutively associated with membrane in unstimulated BEAS-2B cells. cPLA$_2\beta$3 is removed from the membrane by homogenizing BEAS-2B cells with excess EGTA, suggesting that Ca^{2+} plays a role in membrane binding. However, the microscopy data indicate that membrane association of cPLA$_2\beta$3 occurs at resting levels of calcium under conditions in which cPLA$_2\alpha$ is cytosolic. cPLA$_2\alpha$ associates with membrane when intracellular calcium is >120 nM, indicating that the concentration of intracellular calcium in serum-starved unstimulated BEAS-2B cells is below this level (16). In addition to calcium, a variety of other factors could contribute to the constitutive association of cPLA$_2\beta$3 with membrane. Unlike cPLA$_2\alpha$, which exhibits calcium-dependent targeting to Golgi, endoplasmic reticulum, and nuclear membrane, cPLA$_2\beta$3 distinctly associates with mitochondria and early endosomes. It is possible that this membrane association is mediated by protein-protein interactions involving a specific region of cPLA$_2\beta$3. The mechanism responsible for cPLA$_2\beta$3 binding to these sites is not known, but the results suggest a novel role for cPLA$_2\beta$3 in the function of early endosomes and mitochondria. The 100-kDa cPLA$_2\beta$ is widely distributed in human tissues, suggesting that it plays a generalized role in cells. PLA$_2$ enzymes have been implicated in calcium-dependent fusion of endosomes, tubule-mediated trafficking in the secretory and endocytic pathways, and recycling of transferrin and transferrin receptors in different cell types. cPLA$_2\beta$3 is the first PLA$_2$ that has been found to be associated with endosomes in resting cells (57–61).

Acknowledgment—We thank Danielle Burke for technical assistance.

REFERENCES

1. Leslie, C. C. (2004) *Prostaglandins Leukot. Essent. Fatty Acids* **70,** 373–376
2. Six, D. A., and Dennis, E. A. (2000) *Biochim. Biophys. Acta* **1488,** 1–19
3. Funk, C. D. (2001) *Science* **294,** 1871–1875
4. Uozumi, N., Kume, K., Nagase, T., Nakatani, N., Ishii, S., Tashiro, F., Komagata, Y., Maki, K., Ikuta, K., Ouchi, Y., Miyazaki, J., and Shimizu, T. (1997) *Nature* **390,** 618–622
5. Nagase, T., Uozumi, N., Ishii, S., Kume, K., Izumi, T., Ouchi, Y., and Shimizu, T. (2000) *Nat. Immunol.* **1,** 42–46
6. Tabuchi, S., Uozumi, N., Ishii, S., Shimizu, Y., Watanabe, T., and Shimizu, T. (2003) *Acta Neurochir. Suppl.* **86,** 169–172
7. Bonventre, J. V., and Sapirstein, A. (2002) *Adv. Exp. Med. Biol.* **507,** 25–31
8. Bonventre, J. V., Huang, Z., Taheri, M. R., O'Leary, E., Li, E., Moskowitz, M. A., and Sapirstein, A. (1997) *Nature* **390,** 622–625
9. Downey, P., Sapirstein, A., O'Leary, E., Sun, T. X., Brown, D., and Bonventre, J. V. (2001) *Am. J. Physiol.* **280,** F607–F618
10. Song, H., Lim, H., Paria, B. C., Matsumoto, H., Swift, L. L., Morrow, J., Bonventre, J. V., and Dey, S. K. (2002) *Development* **129,** 2879–2889
11. Haq, S., Kilter, H., Michael, A., Tao, J., O'Leary, E., Sun, X. M., Walters, B., Bhattacharya, K., Chen, X., Cui, L., Andreucci, M., Rosenzweig, A., Guerrero, J. L., Patten, R., Liao, R., Molkentin, J., Picard, M., Bonventre, J. V., and Force, T. (2003) *Nat. Med.* **9,** 944–951
12. Dessen, A., Tang, J., Schmidt, H., Stahl, M., Clark, J. D., Seehra, J., and Somers, W. S.

(1999) *Cell* **97,** 349–360
13. Glover, S., de Carvalho, M. S., Bayburt, T., Jonas, M., Chi, E., Leslie, C. C., and Gelb, M. H. (1995) *J. Biol. Chem.* **270,** 15359–15367
14. Nalefski, E. A., Sultzman, L. A., Martin, D. M., Kriz, R. W., Towler, P. S., Knopf, J. L., and Clark, J. D. (1994) *J. Biol. Chem.* **269,** 18239–18249
15. Gijon, M. A., Spencer, D. M., Kaiser, A. L., and Leslie, C. C. (1999) *J. Cell Biol.* **145,** 1219–1232
16. Evans, J. H., Spencer, D. M., Zweifach, A., and Leslie, C. C. (2001) *J. Biol. Chem.* **276,** 30150–30160
17. Pickard, R. T., Strifler, B. A., Kramer, R. M., and Sharp, J. D. (1999) *J. Biol. Chem.* **274,** 8823–8831
18. Song, C., Chang, X. J., Bean, K. M., Proia, M. S., Knopf, J. L., and Kriz, R. W. (1999) *J. Biol. Chem.* **274,** 17063–17067
19. Underwood, K. W., Song, C., Kriz, R. W., Chang, X. J., Knopf, J. L., and Lin, L. L. (1998) *J. Biol. Chem.* **273,** 21926–21932
20. Chiba, H., Michibata, H., Wakimoto, K., Seishima, M., Kawasaki, S., Okubo, K., Mitsui, H., Torii, H., and Imai, Y. (2004) *J. Biol. Chem.* **279,** 12890–12897
21. Ohto, T., Uozumi, N., Hirabayashi, T., and Shimizu, T. (2005) *J. Biol. Chem.* **280,** 24576–24583
22. Clissold, P. M., and Ponting, C. P. (2001) *Trends Biochem. Sci.* **26,** 7–9
23. Sharp, J. D., Pickard, R. T., Chiou, X. G., Manetta, J. V., Kovacevic, S., Miller, J. R., Varshavsky, A. D., Roberts, E. F., Strifler, B. A., and Brems, D. N. (1994) *J. Biol. Chem.* **269,** 23250–23254
24. Pickard, R. T., Chiou, X. G., Strifler, B. A., DeFelippis, M. R., Hyslop, P. A., Tebbe, A. L., Yee, Y. K., Reynolds, L. J., Dennis, E. A., Kramer, R. M., and Sharp, J. D. (1996) *J. Biol. Chem.* **271,** 19225–19231
25. Ghomashchi, F., Stewart, A., Hefner, Y., Ramanadham, S., Turk, J., Leslie, C. C., and Gelb, M. H. (2001) *Biochim. Biophys. Acta* **1513,** 160–166
26. Connolly, S., Bennion, C., Botterell, S., Croshaw, P. J., Hallam, C., Hardy, K., Hartopp, P., Jackson, C. G., King, S. J., Lawrence, L., Mete, A., Murray, D., Robinson, D. H., Smith, G. M., Stein, L., Walters, I., Wells, E., and Withnall, W. J. (2002) *J. Med. Chem.* **45,** 1348–1362
27. Mounier, C. M., Ghomashchi, F., Lindsay, M. R., James, S., Singer, A. G., Parton, R. G., and Gelb, M. H. (2004) *J. Biol. Chem.* **279,** 25024–25038
28. Stewart, A., Ghosh, M., Spencer, D. M., and Leslie, C. C. (2002) *J. Biol. Chem.* **277,** 29526–29536
29. Leslie, C. C., and Gelb, M. H. (2004) *Methods Mol. Biol.* **284,** 229–242
30. de Carvalho, M. G., Garritano, J., and Leslie, C. C. (1995) *J. Biol. Chem.* **270,** 20439–20446
31. Lindbom, J., Ljungman, A. G., Lindahl, M., and Tagesson, C. (2002) *J Interferon Cytokine Res.* **22,** 947–955
32. Ghomashchi, F., Loo, R., Balsinde, J., Bartoli, F., Apitz-Castro, R., Clark, J. D., Dennis, E. A., and Gelb, M. H. (1999) *Biochim. Biophys. Acta* **1420,** 45–56
33. Collins, T. J., Berridge, M. J., Lipp, P., and Bootman, M. D. (2002) *EMBO J.* **21,** 1616–1627
34. Shah, M., Patel, K., Mukhopadhyay, S., Xu, F., Guo, G., and Sehgal, P. B. (2006) *J. Biol. Chem.* **281,** 7302–7308
35. Dugast, M., Toussaint, H., Dousset, C., and Benaroch, P. (2005) *J. Biol. Chem.* **280,** 19656–19664
36. Tai, G., Lu, L., Johannes, L., and Hong, W. (2005) *Methods Enzymol.* **404,** 442–453
37. Horiuchi, T., and Aigaki, T. (2006) *Biol. Cell* **98,** 135–140
38. Su, Z., Wang, J., Yu, J., Huang, X., and Gu, X. (2006) *Genome Res.* **16,** 182–189
39. Pan, Q., Bakowski, M. A., Morris, Q., Zhang, W., Frey, B. J., Hughes, T. R., and Blencowe, B. J. (2005) *Trends Genet.* **21,** 73–77
40. Cartegni, L., and Krainer, A. R. (2003) *Nat. Struct. Biol.* **10,** 120–125
41. Yuan, Z. A., Chen, E., and Gibson, C. W. (2001) *DNA Cell Biol.* **20,** 807–813
42. Hide, W. A., Babenko, V. N., van Heusden, P. A., Seoighe, C., and Kelso, J. F. (2001) *Genome Res.* **11,** 1848–1853
43. Sugnet, C. W., Srinivasan, K., Clark, T. A., O'Brien, G., Cline, M. S., Wang, H., Williams, A., Kulp, D., Blume, J. E., Haussler, D., and Ares, M. (2006) *PLoS Comput. Biol.* **2,** e4
44. Trewick, S. C., McLaughlin, P. J., and Allshire, R. C. (2005) *EMBO Rep.* **6,** 315–320
45. Ayoub, N., Noma, K., Isaac, S., Kahan, T., Grewal, S. I., and Cohen, A. (2003) *Mol. Cell. Biol.* **23,** 4356–4370
46. Lancaster, D. E., McDonough, M. A., and Schofield, C. J. (2004) *Biochem. Soc. Trans.* **32,** 943–945
47. Elkins, J. M., Hewitson, K. S., McNeill, L. A., Seibel, J. F., Schlemminger, I., Pugh, C. W., Ratcliffe, P. J., and Schofield, C. J. (2003) *J. Biol. Chem.* **278,** 1802–1806
48. Nalefski, E. A., and Falke, J. J. (1996) *Protein Sci.* **5,** 2375–2390
49. Clark, J. D., Lin, L. L., Kriz, R. W., Ramesha, C. S., Sultzman, L. A., Lin, A. Y., Milona, N., and Knopf, J. L. (1991) *Cell* **65,** 1043–1051
50. Jimenez, J. L., Smith, G. R., Contreras-Moreira, B., Sgouros, J. G., Meunier, F. A., Bates, P. A., and Schiavo, G. (2003) *J. Mol. Biol.* **333,** 621–639
51. Xu, G. Y., McDonagh, T., Yu, H. A., Nalefski, E. A., Clark, J. D., and Cumming, D. A. (1998) *J. Mol. Biol.* **280,** 485–500
52. Perisic, O., Fong, S., Lynch, D. E., Bycroft, M., and Williams, R. L. (1998) *J. Biol. Chem.* **273,** 1596–1604
53. Bittova, L., Sumandea, M., and Cho, W. (1999) *J. Biol. Chem.* **274,** 9665–9672
54. Stahelin, R. V., Rafter, J. D., Das, S., and Cho, W. (2003) *J. Biol. Chem.* **278,** 12452–12460
55. Perisic, O., Paterson, H. F., Mosedale, G., Lara-Gonzalez, S., and Williams, R. L. (1999) *J. Biol. Chem.* **274,** 14979–14987
56. Nalefski, E. A., and Falke, J. J. (1998) *Biochemistry* **37,** 17642–17650
57. Mayorga, L. S., Beron, W., Sarrouf, M. N., Colombo, M. I., Creutz, C., and Stahl, P. D. (1994) *J. Biol. Chem.* **269,** 30927–30934
58. Young, S. P. (2000) *FEBS Lett.* **466,** 135–138
59. Mayorga, L. S., Colombo, M. I., Lennartz, M., Brown, E. J., Rahman, K. H., Weiss, R., Lennon, P. J., and Stahl, P. D. (1993) *Proc. Natl. Acad. Sci. U. S. A.* **90,** 10255–10259
60. de Figueiredo, P., Doody, A., Polizotto, R. S., Drecktrah, D., Wood, S., Banta, M., Strang, M. S., and Brown, W. J. (2001) *J. Biol. Chem.* **276,** 47361–47370
61. Chan, D., Strang, M., Judson, B., and Brown, W. J. (2004) *Mol. Biol. Cell* **15,** 1871–1880